

The H^+ related defects involved in domain reversal for both near-stoichiometric and heavily Mg-doped lithium niobate crystals

W. Yan^{1,a}, Y. Kong¹, L. Shi¹, J. Yao², S. Chen¹, L. Sun¹, D. Zhao¹, J. Xu², and G. Zhang²

¹ R&D Center for Photon-Electro materials, Nankai University, Tianjin 300071, China

² Photonics Center, College of Physical Science, Nankai University, Tianjin 300071, China

Received 27 July 2004

Published online 15 March 2005 – © EDP Sciences, Società Italiana di Fisica, Springer-Verlag 2005

Abstract. Domain reversal was performed on both near-stoichiometric and heavily Mg-doped lithium niobate crystals. H^+ related defect structures in these two types of crystals were studied through the infrared absorption spectra. It is found that the intensity of some decomposed peaks of absorption band change apparently during domain reversal for near-stoichiometric lithium niobate crystals but not for heavily Mg-doped lithium niobate crystals. According to these experimental results, distinct models about H^+ related defect structure in $LiNbO_3$ lattice were supposed for them. Nb_{Li}^{4+} and Mg_{Nb}^{3-} were considered as the centers of H^+ related defect complex for near-stoichiometric and heavily Mg-doped lithium niobate crystals respectively. Different behavior of them was used to explain the difference of infrared absorption spectra during domain reversal between two types of crystals.

PACS. 78.30.-j Absorption spectra – 61.50.Nw Crystal stoichiometry – 61.72.Ji Point defects

1 Introduction

Lithium niobate ($LiNbO_3$, LN) is an outstanding material with wide applications in modulators, waveguides, frequency doubling, second harmonic generation, high-density storage, etc. Many physical and chemical properties of $LiNbO_3$ depend on the doping ions and the stoichiometry of crystal. Recently, near-stoichiometric LN and Mg-doped LN become the focus of research for their enhanced performance in the optical application. Various defects in crystal, especially intrinsic and impurity defects, govern the optical properties of crystal. More and more work has been done on the analysis of these defect structures [1,2]. Nonetheless, the discussion about this topic has continued for a long time.

Hydrogen is present in nearly all ABO_3 compounds, it forms an OH^- impurity complex and has an influence on the chemical and physical applications. The OH^- stretching vibration is sensitive to the change of the around ion environment and the OH^- absorption spectra can be used as a probe for defect structure. The infrared absorption band associated to the OH^- stretching vibration in $LiNbO_3$ first reported by Smith et al. [3] in 1968. From then on, a lot of work on this subject has been done. For basic understanding of this topic, we refer readers to the extensive literature [4,5].

Gopalan et al. [6] have investigated domain reversal on CLN crystal and observed its infrared absorption spectra change. In order to explain their experimental results, the Nb-vacancy model was employed. But many experimental results have proved that the Li-vacancy model is more suitable [7–9]. On the other hand, Lengyel et al. [18] also demonstrate the infrared spectra change in time at 80–120 °C, which thanks to the high stoichiometry of $LiNbO_3$ sample. In this study, the H^+ related defects of near-stoichiometric LN and Mg-doped LN samples are investigated by domain reversal, Li-vacancy model employed to explain the change of infrared absorption spectra.

2 Experimental procedure

Congruent $LiNbO_3$ and heavily Mg-doped Single crystals were grown along z -axis in air by the Czochralski technique at the R&D Center for Photon-Electro Materials of Nankai University. The congruent composition was determined to be 48.4 mol% Li_2O and 51.6 mol% Nb_2O_5 , and the composition of heavily Mg-doped Single crystal be 6.0 mol% MgO . The as-grown crystals were cut to rectangular-shaped plates of $20 \times 20 \times 0.5(z)$ (mm^3). The vapor transport equilibrant (VTE) technique [11] was employed to improve the $[Li]/[Nb]$ ratios of these z -cut congruent plates. Each VTE sample was polished to characterize its composition by measuring the width

^a e-mail: fls@mail.nankai.edu.cn

of a few Raman lines [17]. In our experiment, three near-stoichiometric samples were investigated, which had 49.5 mol%, 49.7 mol% and 49.9 mol% Li_2O in the crystal. These samples and another heavily Mg-doped sample are labelled as L49.5, L49.7, L49.9 and L6.0, respectively.

The infrared absorption spectra of these plates were measured by a Nicolet-701 FT-IR spectrometer with a resolution of $\pm 0.5 \text{ cm}^{-1}$. The incident light beam passes through the plate along the z -axis, with the light polarization perpendicular to c -axis. Following this, domain reversal was carried out on these samples at room temperature by applying a DC field across the crystal thickness. The poling fields were about 5, 3, 2 and 7 kV/mm corresponding to sample L49.5, L49.7, L49.9 and L6.0. The infrared absorption spectra of these domain-reversed samples were measured again. Then, the near-stoichiometric samples were annealed at $200 \text{ }^\circ\text{C}$ for 100 min. It is reported by Gopalan et al. [6] that annealing above $200 \text{ }^\circ\text{C}$ can make the internal field realign parallel to the new polarization direction quickly. After the samples cooled down to room temperature, their absorption spectra were thirdly measured.

3 Results and discussion

Firstly, the hydrogen concentrations of our NSLN samples are determined from the absorption spectra. Here, we follow the method used by Klauer et al. to calculate the hydrogen concentration [14]. In their work, the hydrogen concentration was given by:

$$c_H = \frac{A_{int,H}}{(\ln 10)a_H} \quad (1)$$

where a_H is the absorption strength per ion and

$$A_{int,H} = \int \alpha_H(\nu) d\nu \quad (2)$$

are the integral of the absorption coefficient $\alpha_H(\nu)$ for OH^- bands, which can be obtained from the absorption spectra. Using the value of a_H , which was estimated to be $(9.125 \pm 1.369) \times 10^{-18} \text{ cm}$ by Klauer et al., the hydrogen concentrations of our samples under three status are calculated from equation (1). From the results, it is apparent that our experiment procedures will not affect the hydrogen concentration of one sample significantly.

Then, these measured curves of absorption spectra were smoothed to suppress the noise. In order to diminish the influence of experimental conditions, the absorption spectra were normalized by the following formula:

$$A'(\nu) = \frac{c}{\int A(\nu) d\nu} \times A(\nu) \quad (3)$$

where, A' and A are absorption intensities before and after normalization and functions of wavenumber ν , and C is a constant. For the invariability of the hydrogen concentration in the sample during the whole experiment, the

normalization of absorption spectra is considered to be reasonable.

The normalized absorption spectra of our samples are shown in Figures 1a, b, c, d corresponding to samples L49.5, L49.7, L49.9 and L6.0, and the dash, solid and dot curves denote different sample status of virgin, domain-reversed, and heat-treated, respectively. From Figures 1a, b, c, we can see that the three decomposed peaks of the absorption band for near-stoichiometric LN crystals become more obvious with the increase of Li composition from 49.7 mol% to 49.9 mol%. These results are in good agreement with the former reports [1,10], so the three-peak model is employed for near-stoichiometric LN crystal in the following discussion.

The absorption spectra of near-stoichiometric and heavily Mg-doped LN crystals were respectively decomposed to three and two Lorentzian peaks by fitting. The fitting results are collected in Table 1, while the results of sample L49.5 and L6.0 are also drawn in Figure 2. Here and later, the peaks of our samples were labelled as L, M and H in the sequence of wavenumber from low to high. For samples L49.5, L49.7 and L49.9, the intensity of peak L after reversal increases by a large amount, peak H almost vanishes, and peak M only slightly decreases (see Tab. 1 and Fig. 2). However, in contrast to near-stoichiometric LN, the intensity of two peaks for sample L6.0 remains unchanged after reversal. Considering the change of H^+ related defect structure can be reflected from the infrared absorption spectra, these experimental results indicate cation environment around H^+ maybe change during domain reversal for near-stoichiometric LN crystal but for heavily Mg-doped LN.

How does the cation environment change for near-stoichiometric LN crystal? To answer this question, we should know firstly the lattice position occupied by H^+ in the crystal. Kong et al. [12] demonstrated that H^+ locates at the longest O-O bonds (336 pm in length) in oxygen triangles nearest to the Li site, substituting Li^+ in the same time. In other words, H^+ occupies V_{Li}^- in the crystal. We also know that V_{Li}^- prefers to charge-compensate $\text{Nb}_{\text{Li}}^{4+}$. So the cation environment around H^+ is related to the intrinsic defect complex of $\text{Nb}_{\text{Li}}^{4+}$ and V_{Li}^- . It is reported that this defect complex reverses by two steps in the domain reversal of LN [13]. Firstly, $\text{Nb}_{\text{Li}}^{4+}$ moves to the neighboring octahedron through the close-packed oxygen plane, but the arrangement of V_{Li}^- doesn't change immediately because of the lack of lithium mobility at room temperature. Then, V_{Li}^- around the original $\text{Nb}_{\text{Li}}^{4+}$ rearranges around the new anti-site position to reach the stable defect equilibrium state. The second step may last a month, but annealing above $200 \text{ }^\circ\text{C}$ can promote it [6]. After the treatment, the internal field will realign parallel to the new P_s , but this step can not affect the value of P_s obviously. Additionally, Klauer et al. [14] have measured an activation energy of 1.23 eV independent of the electric field up to 10^7 V/m , which suggested that H^+ still locates at V_{Li}^- without any movement even under very high electric field.

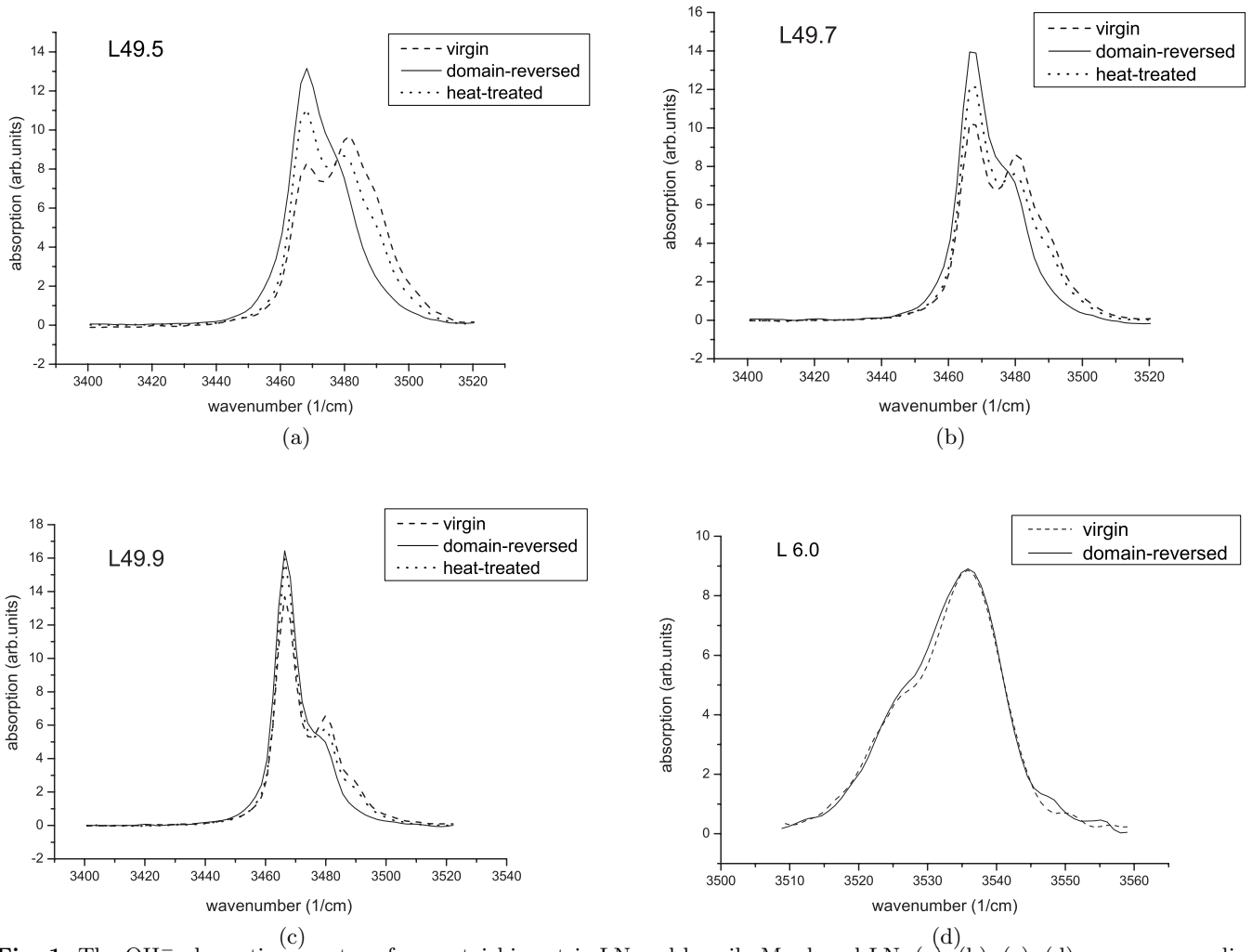


Fig. 1. The OH^- absorption spectra of near-stoichiometric LN and heavily Mg-doped LN: (a), (b), (c), (d) are corresponding to samples L49.5, L49.7, L49.9 and L6.0; the dash, solid and dot curve denote different sample status of virgin, domain-reversed, and heat-treated, respectively.

Table 1. The position and intensity of component peaks in the OH^- absorption spectra of samples: (I) virgin, (II) domain-reversed and (III) heat-treated.

Sample	Position of peak (cm^{-1})			Intensity of peak (arb. units)		
	L	M	H	L	M	H
L49.5 (I)	3467.8	3480.5	3489.8	6.0	7.5	3.2
L49.5 (II)	3467.5	3477.4		10.5	6.5	
L49.5 (III)	3467.6	3479.5	3489.3	9.0	6.6	2.3
L49.7 (I)	3467.2	3480.2	3490.2	8.7	7.2	1.8
L49.7 (II)	3467.2	3478.0		12.4	6.1	
L49.7 (III)	3467.3	3479.6	3489.8	10.6	6.2	1.3
L49.9 (I)	3466.7	3479.9	3489.9	13.1	5.3	0.9
L49.9 (II)	3466.7	3478.3		16.1	3.9	
L49.9 (III)	3466.7	3479.4	3490.7	15.0	4.7	0.5
L6.0 (I)	3526.5	3536.1		2.9	8.1	
L6.0 (II)	3525.7	3536.1		3.4	8.6	

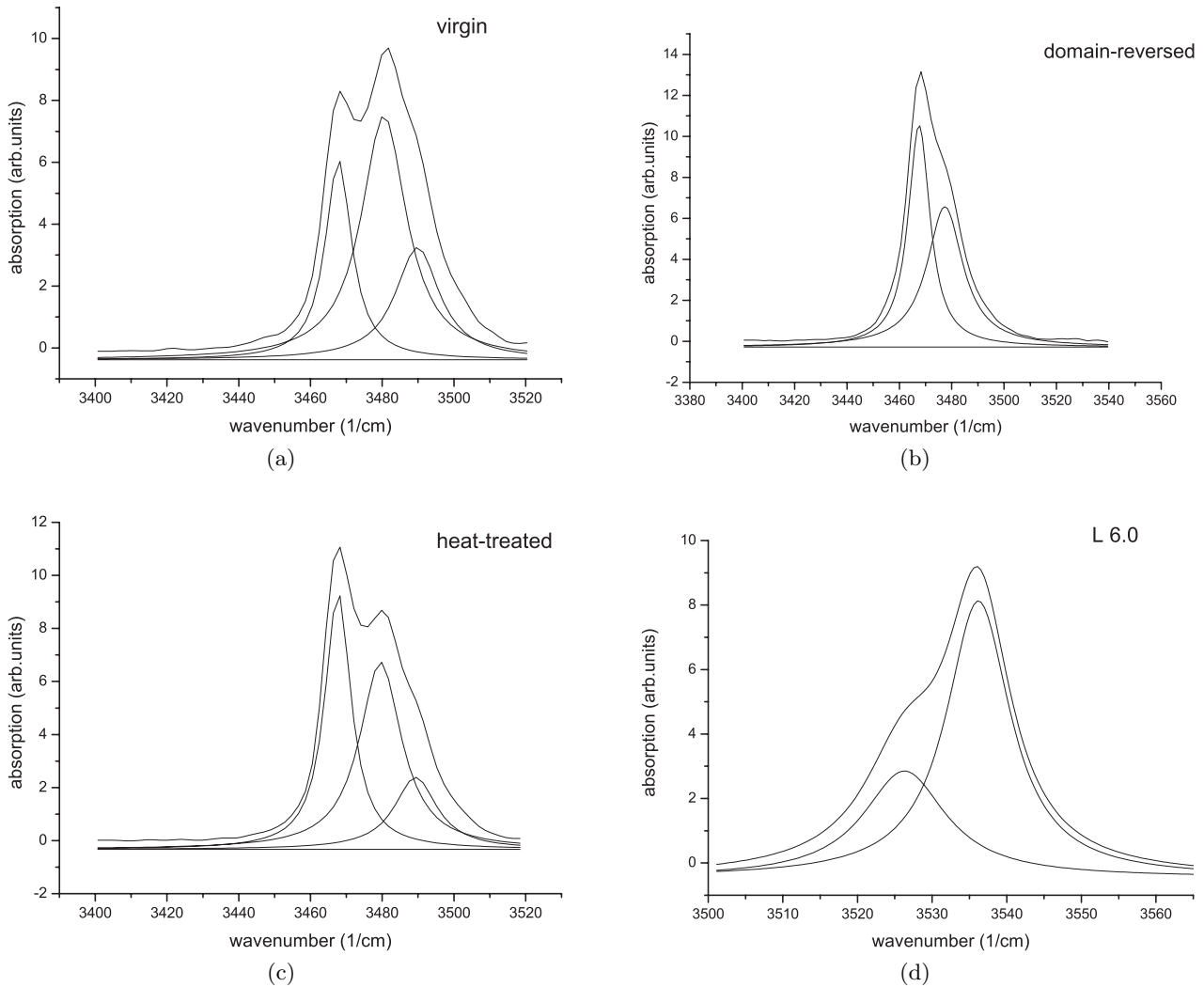


Fig. 2. The components of OH^- absorption spectra of sample L49.5 and L6.0: (a), (b), (c) are corresponding to spectra virgin, domain-reversed, and heat-treated status for L49.5; (d) corresponding to spectra virgin status for L6.0.

Therefore, we consider that H^+ doesn't move during domain reversal and the movement of $\text{Nb}_{\text{Li}}^{4+}$ causes the change of cation environment. In comparison with the pure LN crystal, a great deal of Mg-related impurity defects rather than intrinsic defects present in heavily Mg-doped LN crystal. Different reversal mechanism of the defects, involving a new type of cation environment around H^+ , is expected for heavily Mg-doped LN crystal in the last several paragraphs.

In the following paragraphs, we shall discuss on the assignment of three decomposed peaks for near-stoichiometric LN and show how does the change of cation environment influence the peak intensity of absorption spectra. Kong et al. proposed that the low wavenumber peak is corresponding to protons directly substituting Li^+ ions, the middle and high wavenumber peaks to protons occupying intrinsic defects V_{Li}^- near $\text{Nb}_{\text{Li}}^{4+}$ and two different ion environments cause these two absorption peaks [1]. Their propose is strongly supported by the experimental result of Grone and Kapphan [15]. They

found that only a very narrow OH^- absorption bands near 3466 cm^{-1} (halfwidth less than 3 cm^{-1}) can be detected if the crystal composition is stoichiometric but H^+ enters the crystal lattice through ion exchange. So, it is generally believed that peak L (about 3466 cm^{-1}) is related to protons directly substituting Li^+ ions and located at 336 pm O-O bonds in oxygen triangles nearest to the Li site, and that Peaks M and H are due to the stretching vibration of OH^- affected by $\text{Nb}_{\text{Li}}^{4+}$.

Figure 3 shows the structure of H^+ related defects in the near-stoichiometric LN, where Figure 3(a) along an oxygen plane, 3(b) perpendicular the c -axis and 3(c) three-dimension view. Position B and C are the nearest and the next nearest Li-sites around $\text{Nb}_{\text{Li}}^{4+}$ to provide V_{Li}^- . Kong et al. proposed that the high wavenumber peak is corresponding to position B and the middle wavenumber peak to position C [1]. In view of their point, when $\text{Nb}_{\text{Li}}^{4+}$ ion moves through the adjacent close-packed oxygen plane to the nearly symmetrical site within the neighboring vacant oxygen octahedra in the first step of domain reversal,

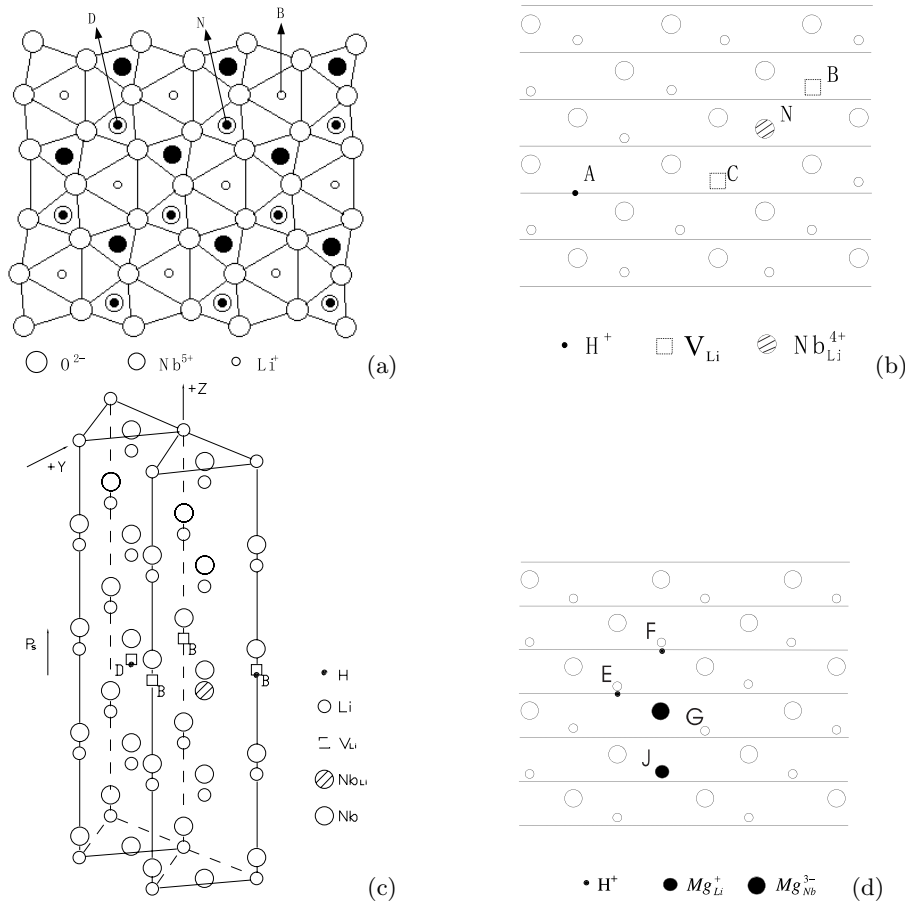


Fig. 3. Structural schematics of LiNbO_3 lattice. (a) along a oxygen plane, white Nb^{5+} and Li^+ symbols corresponding to ions above plane, black symbols to ions below plane. Position N corresponds to the site of $\text{Nb}_{\text{Li}}^{4+}$, position B, D correspond to the sites of V_{Li}^- , on which H^+ locates and arises the absorption peak M, H. (P_s points out of plane). (b), (d) perpendicular the c -axis. Position D doesn't locate on the same plane with position A, B, C, N. (c) three-dimension view. (a), (b), (c) are for near-stoichiometric LN and (d) for heavily Mg-doped LN.

$\text{Nb}_{\text{Li}}^{4+}$ ion will be separated from position B by the oxygen plane and closer to position C than before. Thus, we can imagine that the cation environment of B and C exchange under this condition (only consider the influence of $\text{Nb}_{\text{Li}}^{4+}$ on the cation environment). So, after domain reversal, the intensities of peaks M and H should also exchange. But we don't find this phenomenon in our experiments. Therefore, the lattice position of V_{Li}^- round $\text{Nb}_{\text{Li}}^{4+}$ should be considered over again. Additionally, it is well known that there is a spontaneous polarization P_s in LiNbO_3 crystal. This P_s may force V_{Li}^- in position C to depart from $\text{Nb}_{\text{Li}}^{4+}$ in the $-P_s$ direction. Moreover, the close-packed oxygen plane just under $\text{Nb}_{\text{Li}}^{4+}$ shown in Figure 3b weakens the electric interaction of $\text{Nb}_{\text{Li}}^{4+}$ and V_{Li}^- , which makes them combine difficultly. Therefore, any V_{Li}^- occurs in this position is unstable.

Which position does the V_{Li}^- corresponding to peak M and L locate at? During domain reversal, we notice that the intensity of peak M only changes a little. This indicates that the corresponding Li vacancy should locate at the position, on which $\text{Nb}_{\text{Li}}^{4+}$ almost has the same influence after domain reversal as before. From Figures 3a

and c, we can see that position D is in the same horizontal plane with $\text{Nb}_{\text{Li}}^{4+}$ and maybe a more suitable position for V_{Li}^- . We consider that this position may correspond to peak M. As far as peak H, position B should be responsible for it. V_{Li}^- in position B is affected more deeply by $\text{Nb}_{\text{Li}}^{4+}$ than that in position D, which leads to more severe distortion of the lattice in position B and makes peak H (about 3489 cm^{-1}) deviate more largely from 3466 cm^{-1} than peak M (about 3481 cm^{-1}). In LN crystal, the amount of H^+ ($10^8 \sim 10^9/\text{cm}^3$) is much less than that of V_{Li}^- ($10^{20} \sim 10^{22}/\text{cm}^3$) and H^+ with positive charge prefers to locate far from $\text{Nb}_{\text{Li}}^{4+}$. In LN crystals with high Li composition, e.g. sample L49.9, V_{Li}^- in position A dominates the intrinsic defects and the amount of H^+ in this position is very large in comparison with the other two position, which lead to the high intensity of peak L. However, the defect complex with two V_{Li}^- around $\text{Nb}_{\text{Li}}^{4+}$ increases by a large amount in the low stoichiometric LN crystals. And H^+ has more chances to occupy in V_{Li}^- position B and C. Thus, peak M and H gain considerable intensity in sample L49.7 and L49.5. V_{Li}^- in position C is closer to $\text{Nb}_{\text{Li}}^{4+}$ than position B, which results in less amount of

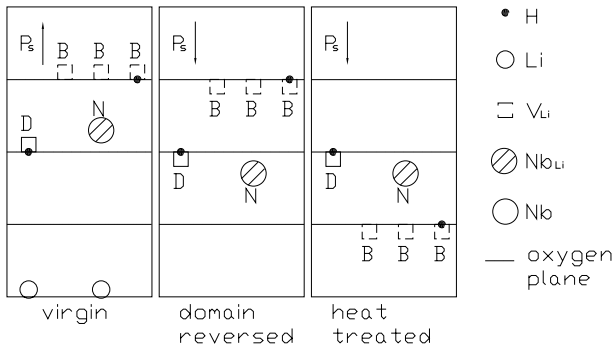


Fig. 4. The sketch of the movement of H^+ related defects in near-stoichiometric LN during domain reversal (view from $+y$ in Fig. 3c). Three parts are corresponding virgin, domain-reversed, heat-treated status. Li vacancies not in the vertical plane are drawn with dot line.

H^+ in position C and the lower intensity of peak H than peak M (see Fig. 2a).

In Figure 4, we show the sketch of the movement of H^+ related defects in this model during domain reversal. The change of absorption spectra can be explained properly. During domain reversal, Nb_{Li}^{4+} ion moves through the adjacent close-packed oxygen plane to the nearly symmetrical site within the neighboring vacant oxygen octahedra, which leaves V_{Li}^- in position B far from Nb_{Li}^{4+} , and the influence of Nb_{Li}^{4+} on V_{Li}^- in position B is largely screened by the oxygen plane. This process makes V_{Li}^- in position B less affected by Nb_{Li}^{4+} , namely, the lattice in position B becomes perfect (equivalent to position A). An equivalent way of thinking of this is that the amount of H^+ in position B decreases nearly to zero but that in position A increases largely. So, the intensity of peak L goes up while peak H almost vanishes from the spectra after domain reversal (see Fig. 2b). The movement of Nb_{Li}^{4+} is almost symmetrical to position D and no large intensity change occurs on peak M. During heat treatment, the mobility of H^+ and V_{Li}^- increases largely especially near intrinsic defects. Thus both of them migrate, rearrange and finally reach the stable defect equilibrium state, which makes the absorption spectra partly recover (see Fig. 2c). It seems not consistent with the result obtained by Lengyel et al. [18]. However, they pointed that only H^+ migrates among lattice sites during the heat treatment, which differs from our case in domain-reversed crystal.

Not apparent shape change of the absorption spectra can be observed during domain reversal for heavily Mg-doped LN, which may be due to large number of Mg-related defects in crystal. When the doping concentrations of Mg reach the first threshold $LiNbO_3$ crystals (5.3 mol% MgO in melt), $Nb_{Li}^{4+}-V_{Li}^-$ defect complex has disappeared, Mg ions enter Nb-sites, and Mg-related impurity defects such as Mg_{Nb}^{3-} and Mg_{Li}^+ begin to dominate in the crystal [16]. For the balance of electric charge, Mg_{Nb}^{3-} may attract Mg_{Li}^+ and H^+ in crystal to form a new defect complex. Figure 3d shows a hypothetical model for this defect complex as comprising a Mg_{Nb}^{3-} surrounded by two H^+

and one Mg_{Li}^+ in the nearest neighborhood. In this model, H^+ locates at the longest O-O bonds as suggested by Kong et al. [12], but they don't substitute the Li ions because of the negative of Mg_{Nb}^{3-} and the diminishing of V_{Li}^- . Just like the case in near-stoichiometric LN, the infrared absorption spectra of heavily Mg-doped LN lie on the location of H^+ . Among the four positions round Mg_{Nb}^{3-} labelled E, F, G and J in Figure 3d, both E, G and F, J are almost equivalent sites for due to their symmetries relative to Mg_{Nb}^{3-} . Though the distribution of H^+ in E, F, G, J positions given in Figure 3d is one likelihood and may be otherwise in fact, there only exist two types of sites for H^+ , corresponding to the two peaks in the infrared absorption spectra (see Fig. 2d). H^+ at the nearest positions of E, G causes the peak M in high wavenumber while slightly far position of F corresponding to the peak L. Considering the participation of Mg_{Li}^+ in the defect complex, different amount of H^+ at two types of sites is expected and leads to different intensity of peak L and M. During domain reversal, Mg_{Nb}^{3-} moves only in the same oxygen octahedral without passing through oxygen plane and the cation environment of H^+ almost remains unchanged, which results in the far less change of absorption spectra.

4 Conclusion

We measure the infrared absorption spectra of virgin, domain-reversed and heat-treated near-stoichiometric LN samples in comparison with heavily Mg-doped LN. By analyzing the intensity of the component peaks, the H^+ related defect structures in two type of LN crystal were investigated. During domain reversal, the movement of H^+ related defect center (Nb_{Li}^{4+} for near-stoichiometric LN) through close-packed oxygen plane affects the H^+ cation environment and then the infrared absorption peak intensity indirectly, which is in contrast with the heavily Mg-doped LN.

This work is partly supported by the National Natural Science Foundation of China (Grant No. 60108001), the National Advanced Materials Committee of China (Grant No. 2001AA313020), and China Basic Research Project (Grant No. 1999033004). The authors are indebted to the referees for their valuable comments.

References

- [1] Y. Kong, W. Zhang, X. Chen, J. Xu, G. Zhang, *J. Phys.: Condens. Matter* **11**, 2139 (1999)
- [2] Y. Furukawa, K. Kitamura, S. Takekawa, K. Niwa, Y. Yajima, N. Iyi, I. Mnushkina, P. Guggenheim, J.M. Martin, *J. Cryst. Growth* **211**, 230 (2000)
- [3] R.G. Smith, D.B. Fraser, R.T. Denton, T.C. Rich, *J. Appl. Phys.* **39**, 4600 (1968)
- [4] J.M. Cabrera, J. Olivares, M. Carrascosa, J. Rams, R. Müller, E. Diéguez, *Adv. Phys.* **45**, 349 (1996)

- [5] M. Wöhlecke, L. Kovács, *Critical Reviews in Solid State and Materials Sciences* **26**, 1 (2001)
- [6] V. Gopalan, M.C. Gupta, *J. Appl. Phys.* **80**, 6099 (1996)
- [7] N. Iyi, K. Kitamura, F. Izumi, J.K. Yamamoto, T. Hayashi, H. Asano, S. Kimura, *J. Solid. State. Chem.* **101**, 340 (1992)
- [8] S. Kojima, *Jpn J. Appl. Phys. Part 1* **32**, 4373 (1993)
- [9] J. Blumel, E. Born, T. Metzger, *J. Phys. Chem. Solids* **55**, 589 (1994)
- [10] K. Polgár, A. Peter, L. Kovács, G. Corradi, Z. Szaller, *J. Cryst. Growth* **177**, 211 (1997)
- [11] R.L. Holman, in *Processing of Crystalline Ceramics*, edited by H. Palmour, R.F. Davis, T.M. Hare (Plenum, New York, 1978), p. 343
- [12] Y. Kong, J. Xu, W. Zhang, G. Zhang, *J. Phys. Chem. Solids* **61**, 1331 (2000)
- [13] S. Kim, V. Gopalan, K. Kitamura, Y. Furukawa, *J. Appl. Phys.* **90**, 2949 (2001)
- [14] S. Klauer, M. Wöhlecke, S. Kapphan, *Phys. Rev. B* **45**, 2786 (1992)
- [15] A. Grone, S. Kapphan, *J. Phys. Chem. Solids* **56**, 687 (1995)
- [16] J. Liu, W. Zhang, G. Zhang, *Phys. Stat. Sol. (a)* **156**, 285 (1996)
- [17] M. Wöhlecke, G. Corradi, K. Betzler, *Appl. Phys. B* **63**, 323 (1996)
- [18] K. Lengyel, L. Kovács, G. Mandula, R. Rupp, *Ferroelectrics* **257**, 255 (2001)